REPORT DOCUMENTATION PAGE

Form Approved OMB No. 0704-0188

1. REPORT DATE *(DD-MM-YYYY)*	2. REPORT TYPE	3. DATES COVERED *(From - To)*
	Technical Papers	

4. TITLE AND SUBTITLE

5a. CONTRACT NUMBER

5b. GRANT NUMBER

5c. PROGRAM ELEMENT NUMBER

6. AUTHOR(S)

5d. PROJECT NUMBER
2303

5e. TASK NUMBER
M2C8

5f. WORK UNIT NUMBER

7. PERFORMING ORGANIZATION NAME(S) AND ADDRESS(ES)

Air Force Research Laboratory (AFMC)
AFRL/PRS
5 Pollux Drive
Edwards AFB CA 93524-7048

8. PERFORMING ORGANIZATION REPORT

9. SPONSORING / MONITORING AGENCY NAME(S) AND ADDRESS(ES)

Air Force Research Laboratory (AFMC)
AFRL/PRS
5 Pollux Drive
Edwards AFB CA 93524-7048

10. SPONSOR/MONITOR'S ACRONYM(S)

11. SPONSOR/MONITOR'S NUMBER(S)

12. DISTRIBUTION / AVAILABILITY STATEMENT

Approved for public release; distribution unlimited.

13. SUPPLEMENTARY NOTES

14. ABSTRACT

11121 008

15. SUBJECT TERMS

16. SECURITY CLASSIFICATION OF:			17. LIMITATION OF ABSTRACT	18. NUMBER OF PAGES	19a. NAME OF RESPONSIBLE PERSON
a. REPORT	b. ABSTRACT	c. THIS PAGE			Leilani Richardson
Unclassified	Unclassified	Unclassified	A		19b. TELEPHONE NUMBER *(include area code)* (661) 275-5015

62 Separate items are enclosed

93ABW208 TP-FY99-0038

✓ Spreadsheet
✓ DTS

MEMORANDUM FOR PRR (Contractor Publication)

6 Jan 1999

FROM: PROI (TI) (STINFO)

SUBJECT: Authorization for Release of Technical Information, Control Number: AFRL-PR-ED-TP-FY99-0038
Karl Christe and Jerry Boatz "On the Existence of the Halocarbonyl and Trifluoromethyl Cations in the Condensed Phase"

Journal submission

(Statement A)

On the Existence of the Halocarbonyl and Trifluoromethyl Cations in the Condensed Phase

K.O. Christe,[*,#,§] B. Hoge,[#,†] J. A. Boatz,[§] G. K. S. Prakash,[#] G. A. Olah,[#] J. A. Sheehy[§]

Loker Hydrocarbon Research Institute, University of Southern California, Los Angeles, California 90089 and Air Force Research Laboratory, Edwards AFB, California 93524

Abstract

Vibrational and multinuclear NMR spectroscopy were used to reexamine previous claims, which were based solely on ^{13}C-NMR spectra, for the existence of the FCO^+ and $ClCO^+$ cations in the condensed phase. The previously reported ^{13}C-NMR signal, observed in the protolytic ionization of *tert*-butyl fluoro-formate and attributed to FCO^+, could not be reproduced. Furthermore, there was no evidence for the formation of FCO^+, when F_2CO was reacted either with solid SbF_5 matrices or with AsF_5 or SbF_5 in SO_2ClF solutions at low-temperatures. The only observable products were the known oxygen-bridged donor-acceptor adducts between F_2CO and the Lewis acids. Similarly, for Cl_2CO or ClFCO and stoichiometric amounts of Lewis acids, only the corresponding oxygen-bridged donor-acceptor adducts were observed. However, in the presence of a two-fold excess of SbF_5, the thermally unstable, ionic salt, $ClCO^+$ $Sb_3F_{16}^-$, could be isolated. The $ClCO^+$ cation was characterized by vibrational spectroscopy and theoretical calculations. Frenking's natural bond orbital (NBO) analysis for CF_3^+ and related species, which contain only one type of p(π) back-donating ligands, was extended to systems containing two types of competing, p(π) back-donating ligands. It is shown that p(π) back-donation increases in the order F<Cl<O for the XCO^+ (X=F or Cl) cations, resulting in C≡O triple bonds, while σ-donation suppresses generation of a positive charge on oxygen. Born-Haber cylces were calculated for the SbF_6^- salts of CF_3^+, FCO^+, and $ClCO^+$, as

well as $ClCO^+Sb_3F_{16}^-$. These cycles demonstrate that unfavorable overall thermodynamics, rather than p(π) back-donation, are the main reasons for the elusiveness of CF_3^+ and FCO^+ salts in the condensed phase. For the F_2CO/SbF_5 system, the overall thermodynamics are also responsible for the preferential formation of an oxygen-bridged donor-acceptor adduct. Potential energy curves were calculated at the B3LYP/SBK+(d) level for the $ClFCO/SbF_5$ and $ClFCO/Sb_3F_{15}$ systems not only to evaluate the relative energies of ionic salts versus covalent donor-acceptor complexes, but also to predict which ligand, i.e., oxygen, fluorine or chlorine, is the preferred donor atom. In excellent agreement with our experimental results, these model calculations show for the $ClFCO/SbF_5$ system a shallow minimum for the oxygen-bridged system, while approaches through the fluorine or chlorine ligands are repulsive. For the $ClFCO/Sb_3F_{15}$ system, the potential for the chlorine ligand approach was again repulsive, while the oxygen-bridged system gave a shallow minimum corresponding to a weak donor-acceptor adduct. The approach through the fluorine ligand resulted in a minimum corresponding to the transfer of a fluoride ion from ClFCO to Sb_3F_{15} with formation of $ClCO^+Sb_3F_{16}^-$. This ionic structure, when corrected for lattice energy effects, becomes energetically more favorable than the oxygen-bridged donor-acceptor adduct.

Introduction

Carbocations play an important role as reactive intermediates in organic synthesis.[1-3] In tricoordinate carbenium ions, the carbon center is usually stabilized by back-donation of a free valence electron pair from a ligand X, which in a simple valence bond description shifts some of the formal positive charge from the carbon center to the ligand X. With increasing

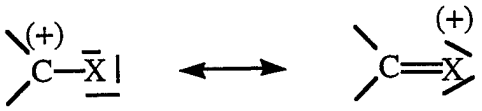

electronegativity, however, the X ligand increasingly resists this electron transfer.[4] Consequently, it is not surprising that condensed phase CF_3^+ is still unknown, although the free cation is vibrationally stable[4] and has been observed by electron impact studies in the gas phase,[5] and the heavier halogen analogues, i.e., CCl_3^+, CBr_3^+ and CI_3^+, have been observed in solution by NMR spectroscopy.[6]

A closely related and challenging problem is the condensed state synthesis of FCO^+. In this cation, two of the fluorine ligands have been replaced by an oxygen atom, which is also highly electronegative, but should be a better p(π) back-donor than fluorine, as shown by the following valence bond structures.

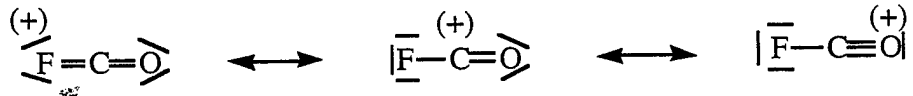

fluoronium oxocarbenium oxonium

The free FCO^+ cation is also vibrationally stable and has previously been characterized by microwave spectroscopy in a liquid-nitrogen-cooled, negative glow discharge.[7] Furthermore, its heavier halogen analogues, $ClCO^+$, $BrCO^+$ and ICO^+, have been observed in SO_2ClF solution by ^{13}C-NMR spectroscopy, but attempts have failed to detect FCO^+ using the same approaches.[8] Very recently, however, a ^{13}C-NMR signal, observed at -78°C in the protolytic ionization of *tert*-butyl fluoroformate with a fivefold excess of FSO_3H/SbF_5, was attributed to FCO^+.[9] It supposedly had been formed by dehydration of protonated fluoroformic acid (1), whose formation was firmly established by ^{13}C-, ^1H-, and ^{19}F- NMR spectroscopy.

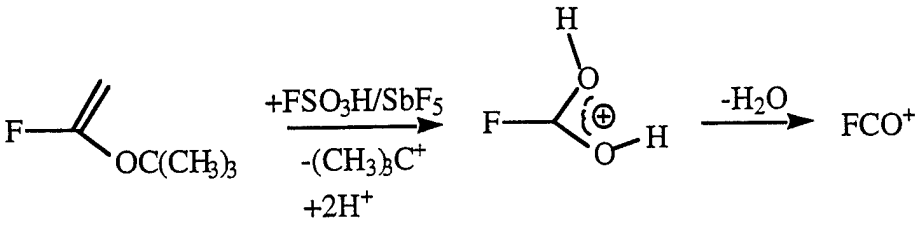

(1)

Since the reported[8,9] experimental evidence for the existence of condensed state FCO^+ and $ClCO^+$ rested exclusively on the observation of ^{13}C-NMR signals in the vicinity of the predicted shift ranges, and F_2CO and Cl_2CO are well known to form the stable oxygen-bridged, donor-acceptor adducts $F_2CO{\cdot}AsF_5$, $F_2CO{\cdot}SbF_5$,[10] and $Cl_2CO{\cdot}AlCl_3$,[11] it was important to reexamine the experimental evidence for the existence of FCO^+ and $ClCO^+$ in the condensed phase. Furthermore, it was interesting to explore under which conditions the oxygen-bridged donor-acceptor adducts and the ionic halocarbonyl salts can be formed and to evaluate the relative contributions of the halogens and oxygen to the electron back-donation in the corresponding carbocations. Another point of interest was the relative donor strength of fluorine, chlorine and oxygen towards strong Lewis acids. Partial results from this study have been presented at two meetings,[12] and a full account is given in this paper.

Experimental Section

Materials and Apparatus. Commercially available phosgene (Matheson), F_2CO (PCR Research Chemicals), AsF_5, and SbF_5 (Ozark Mahoning) were purified by fractional condensation prior to use. Literature methods were used for the syntheses of ClFCO,[13] $Cl_2CO{\cdot}SbF_5$,[14] and *tert*-butyl fluoroformate.[15]

Volatile materials were handled in a stainless-steel vacuum line equipped with Teflon-FEP U-traps, stainless-steel bellows-seal valves and a Heise Bourdon tube-type pressure gauge.[16]

The line and other hardware were passivated with ClF_3 and HF. Nonvolatile materials were handled in the dry nitrogen atmosphere of a glove box.

Vibrational Spectra. Raman spectra were recorded on a Cary Model 83GT with the 488 nm exciting line of a Lexel Model 95 Ar-ion laser, using sealed glass tubes as sample containers. A previously described device[17] was used for recording the low temperature spectra. Infrared spectra were recorded in the range of 4000-300 cm^{-1} on a Midac Model M FTIR spectrometer. For the low temperature spectra, the cold sample was placed inside the glove box between cold AgCl windows, which were mounted in a liquid N_2-cooled copper block, mated with an O-ring flange to an evacuable glass cell with outer CsI windows.

Nuclear Magnetic Resonance Spectroscopy. The NMR spectra were recorded on a Varian Model Unity 300 MHz NMR spectrometer equipped with a 5 mm variable-temperature broad band probe. Sealed capillaries, which were filled with acetone-d_6 as lock substance, TMS as ^{13}C reference, and $CFCl_3$ or $C_6H_5CF_3$ as ^{19}F reference, were placed inside the NMR tubes.

Preparation of [ClCO][Sb_3F_{16}]. On the vacuum line, ClFCO (3.2 mmol) was condensed at -196 °C into a 3/4 inch o.d. Teflon-FEP ampule, which was closed by a steel valve and contained a weighed amount (9.5 mmol) of SbF_5 dissolved in 4 mL of SO_2ClF. The reaction mixture was stirred with a Teflon coated magnetic stirring bar for one hour at –78 °C. After warming the clear colorless solution to –64 °C ($CHCl_3$ slush bath), the gas phase above the liquid did not contain any ClFCO and F_2CO, as shown by infrared spectroscopy. The solvent was pumped off over night at –64 °C. The resulting white powder consisted of [ClCO][Sb_3F_{16}] (2.323 g = 3.15 mmol).

NMR Spectroscopic Characterisation of [ClCO][*cis*-Sb_3F_{16}]. A solution of ClFCO and three equivalents of SbF_5 in SO_2ClF at –60 °C showed only the ^{13}C NMR signal (singlet at 134 ppm)

for the $ClCO^+$ cation. The ^{19}F NMR spectrum exhibited broad multipets in the Sb-F region from –90 to –140 ppm, characteristic for *cis*-$Sb_3F_{16}^-$.[18]

Under the same conditions, a 1:2 mixture of ClFCO and SbF_5 resulted in two ^{13}C-NMR signals: a doublet at 164 ppm (^1J(CF) 383 Hz) for the ClFCO•SbF_5 adduct[14] and a singlet at 134 ppm for the $ClCO^+$ cation. The corresponding ^{19}F-NMR spectrum showed sharp signals (-141.0, -127.7, -112.2, -108.3 and –89.5 ppm) with the coupling pattern characteristic of the *cis*-$Sb_3F_{16}^-$ anion (-141.1, -127.8, -112.4, -108.3, -89.7)[18] and the relative intensities of 2.5 : 1.8 : 7.5 : 2.2 : 2. The ^{19}F spectrum also showed two doublets, a more intense one at –109.6 and a less intense one at –105.2 ppm, which are characteristic of the four equivalent fluorine atoms in the 1:1 complexes, ClFCO•SbF_5 and SO_2ClF•SbF_5, respectively (literature values: -110.0 and –105.1 ppm, respectively)[19]. The quintet resonances, expected for the single axial fluorine atoms of these compounds, were not observed. The ^{19}F resonance, due to the fluorine atom of the ClFCO part of the ClFCO•SbF_5 adduct, was observed at 74 ppm. The value of 59.9 ppm, previously reported[19] for this resonance, is incorrect and is due to free ClFCO.[20]

Protolytic Ionization of *tert*-Butyl Fluoroformate. *Tert*-butyl fluoroformate was added at -196 °C to a frozen, 1 molar solution of a fivefold excess of FSO_3H/SbF_5 (1/1 mole ratio) in SO_2ClF and warmed to –78 °C. After recording the NMR spectra of the intensely yellow solution at –78 °C, the sample was allowed to warm up to room temperature for about 10 min, and the spectra were rerecorded at –78 °C. No signs for either decomposition or any other changes were observed. The spectra exhibited only the previously reported resonances,[9] except for the missing doublet at δ = 117.5 in the ^{13}C spectrum.

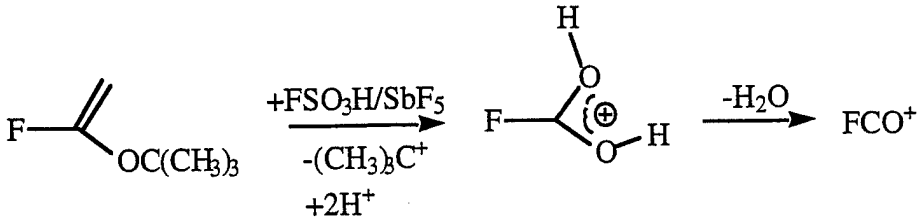

(1)

Since the reported[8,9] experimental evidence for the existence of condensed state FCO^+ and $ClCO^+$ rested exclusively on the observation of ^{13}C-NMR signals in the vicinity of the predicted shift ranges, and F_2CO and Cl_2CO are well known to form the stable oxygen-bridged, donor-acceptor adducts $F_2CO{\cdot}AsF_5$, $F_2CO{\cdot}SbF_5$,[10] and $Cl_2CO{\cdot}AlCl_3$,[11] it was important to reexamine the experimental evidence for the existence of FCO^+ and $ClCO^+$ in the condensed phase. Furthermore, it was interesting to explore under which conditions the oxygen-bridged donor-acceptor adducts and the ionic halocarbonyl salts can be formed and to evaluate the relative contributions of the halogens and oxygen to the electron back-donation in the corresponding carbocations. Another point of interest was the relative donor strength of fluorine, chlorine and oxygen towards strong Lewis acids. Partial results from this study have been presented at two meetings,[12] and a full account is given in this paper.

Experimental Section

Materials and Apparatus. Commercially available phosgene (Matheson), F_2CO (PCR Research Chemicals), AsF_5, and SbF_5 (Ozark Mahoning) were purified by fractional condensation prior to use. Literature methods were used for the syntheses of ClFCO,[13] $Cl_2CO{\cdot}SbF_5$,[14] and *tert*-butyl fluoroformate.[15]

Volatile materials were handled in a stainless-steel vacuum line equipped with Teflon-FEP U-traps, stainless-steel bellows-seal valves and a Heise Bourdon tube-type pressure gauge.[16]

The line and other hardware were passivated with ClF_3 and HF. Nonvolatile materials were handled in the dry nitrogen atmosphere of a glove box.

Vibrational Spectra. Raman spectra were recorded on a Cary Model 83GT with the 488 nm exciting line of a Lexel Model 95 Ar-ion laser, using sealed glass tubes as sample containers. A previously described device[17] was used for recording the low temperature spectra. Infrared spectra were recorded in the range of 4000-300 cm^{-1} on a Midac Model M FTIR spectrometer. For the low temperature spectra, the cold sample was placed inside the glove box between cold AgCl windows, which were mounted in a liquid N_2-cooled copper block, mated with an O-ring flange to an evacuable glass cell with outer CsI windows.

Nuclear Magnetic Resonance Spectroscopy. The NMR spectra were recorded on a Varian Model Unity 300 MHz NMR spectrometer equipped with a 5 mm variable-temperature broad band probe. Sealed capillaries, which were filled with acetone-d_6 as lock substance, TMS as ^{13}C reference, and $CFCl_3$ or $C_6H_5CF_3$ as ^{19}F reference, were placed inside the NMR tubes.

Preparation of [ClCO][Sb_3F_{16}]. On the vacuum line, ClFCO (3.2 mmol) was condensed at -196 °C into a 3/4 inch o.d. Teflon-FEP ampule, which was closed by a steel valve and contained a weighed amount (9.5 mmol) of SbF_5 dissolved in 4 mL of SO_2ClF. The reaction mixture was stirred with a Teflon coated magnetic stirring bar for one hour at –78 °C. After warming the clear colorless solution to –64 °C ($CHCl_3$ slush bath), the gas phase above the liquid did not contain any ClFCO and F_2CO, as shown by infrared spectroscopy. The solvent was pumped off over night at –64 °C. The resulting white powder consisted of [ClCO][Sb_3F_{16}] (2.323 g = 3.15 mmol).

NMR Spectroscopic Characterisation of [ClCO][*cis*-Sb_3F_{16}]. A solution of ClFCO and three equivalents of SbF_5 in SO_2ClF at –60 °C showed only the ^{13}C NMR signal (singlet at 134 ppm)

for the $ClCO^+$ cation. The ^{19}F NMR spectrum exhibited broad multipets in the Sb-F region from –90 to –140 ppm, characteristic for *cis*-$Sb_3F_{16}^-$.[18]

Under the same conditions, a 1:2 mixture of ClFCO and SbF_5 resulted in two ^{13}C-NMR signals: a doublet at 164 ppm (^1J(CF) 383 Hz) for the ClFCO•SbF_5 adduct[14] and a singlet at 134 ppm for the $ClCO^+$ cation. The corresponding ^{19}F-NMR spectrum showed sharp signals (-141.0, -127.7, -112.2, -108.3 and –89.5 ppm) with the coupling pattern characteristic of the *cis*-$Sb_3F_{16}^-$ anion (-141.1, -127.8, -112.4, -108.3, -89.7)[18] and the relative intensities of 2.5 : 1.8 : 7.5 : 2.2 : 2. The ^{19}F spectrum also showed two doublets, a more intense one at –109.6 and a less intense one at –105.2 ppm, which are characteristic of the four equivalent fluorine atoms in the 1:1 complexes, ClFCO•SbF_5 and SO_2ClF•SbF_5, respectively (literature values: -110.0 and –105.1 ppm, respectively)[19]. The quintet resonances, expected for the single axial fluorine atoms of these compounds, were not observed. The ^{19}F resonance, due to the fluorine atom of the ClFCO part of the ClFCO•SbF_5 adduct, was observed at 74 ppm. The value of 59.9 ppm, previously reported[19] for this resonance, is incorrect and is due to free ClFCO.[20]

Protolytic Ionization of *tert*-Butyl Fluoroformate. *Tert*-butyl fluoroformate was added at -196 °C to a frozen, 1 molar solution of a fivefold excess of FSO_3H/SbF_5 (1/1 mole ratio) in SO_2ClF and warmed to –78 °C. After recording the NMR spectra of the intensely yellow solution at –78 °C, the sample was allowed to warm up to room temperature for about 10 min, and the spectra were rerecorded at –78 °C. No signs for either decomposition or any other changes were observed. The spectra exhibited only the previously reported resonances,[9] except for the missing doublet at δ = 117.5 in the ^{13}C spectrum.

Computational Methods.

Vibrational spectra for FCO^+ and $ClCO^+$, as well as the isoelectronic and well-known species FCN and ClCN, were computed using the single- and double-excitation coupled-cluster method[21] with a noniterative treatment of connected triple excitations, denoted CCSD(T),[22] in 6-311+G(2d) atomic basis sets.[23] At the CCSD(T) geometries, isotropic nuclear magnetic resonance shieldings were computed using the GIAO-MBPT(2) approach,[24] which employs the gauge-including atomic orbital (GIAO) solution to the gauge-invariance problem[25] and density matrices obtained from second-order many-body perturbation theory [MBPT(2)]. The ACES II program systems[26] on IBM RS/6000 work stations were used for these calculations.

Natural bond orbital (NBO) analyses[27] of the one-electron density matrices obtained from single- and double-excitation quadratic configuration-interaction (QCISD) calculations[28] were carried out for FCO^+ and $ClCO^+$, as well as for a series of benchmark compounds that included FCN, ClCN, CF_3^+, CCl_3^+, BF_3, and BCl_3. In this approach, the molecular wave function is decomposed through a set of natural bond orbitals into localized bonding, antibonding, and lone-pair units. These computations were carried out using the Gaussian 94 program system.[29]

Constrained geometry optimizations of SbF_5 + ClFCO and Sb_3F_{15} + ClFCO were performed using density functional methods. The B3LYP hybrid functional[30] and the Stevens, Basch, Krauss, Jasien, and Cundari effective core potentials and the corresponding valence double-zeta basis sets[31] were used. The basis set was augmented with a diffuse s+p shell[32] and a single Cartesian d polarization function on each atom.[33] These calculations, hereafter denoted as B3LYP/SBK+(d), were performed using the Gaussian 94 electronic structure program.[29]

CD_3COCD_3), which might have been formed accidentally as a by-product in the original experiment or may have leaked from a capillary used as a standard for the ^{19}F-NMR spectra.

Properties of $ClCO^+Sb_3F_{16}^-$. The $ClCO^+Sb_3F_{16}^-$ salt is a white solid which is thermally stable up to about –10 °C and decomposes to give ClFCO, SbF_5 and some F_2CO and SbF_4Cl resulting from a chlorine-fluorine exchange between ClFCO and SbF_5. This competing halogen exchange reaction prevented the determination of a reliable heat of dissociation from an Arrhenius plot of the vapor pressure-temperature data. The identity of the anion as *cis*-$Sb_3F_{16}^-$ [18] was established by its low-temperature ^{19}F-NMR spectrum in SO_2ClF solution (see Experimental Section). The $ClCO^+$ cation was identified by its ^{13}C-NMR signal of 134 ppm[8] and vibrational spectroscopy (see below).

Vibrational Spectra. Infrared and Raman spectra are ideally suited to distinguish between ionic salts and covalent donor-acceptor adducts.[35] As can be seen from (7), the formation of a halocarbonyl cation from the corresponding carbonyl dihalide results in a strengthening of both

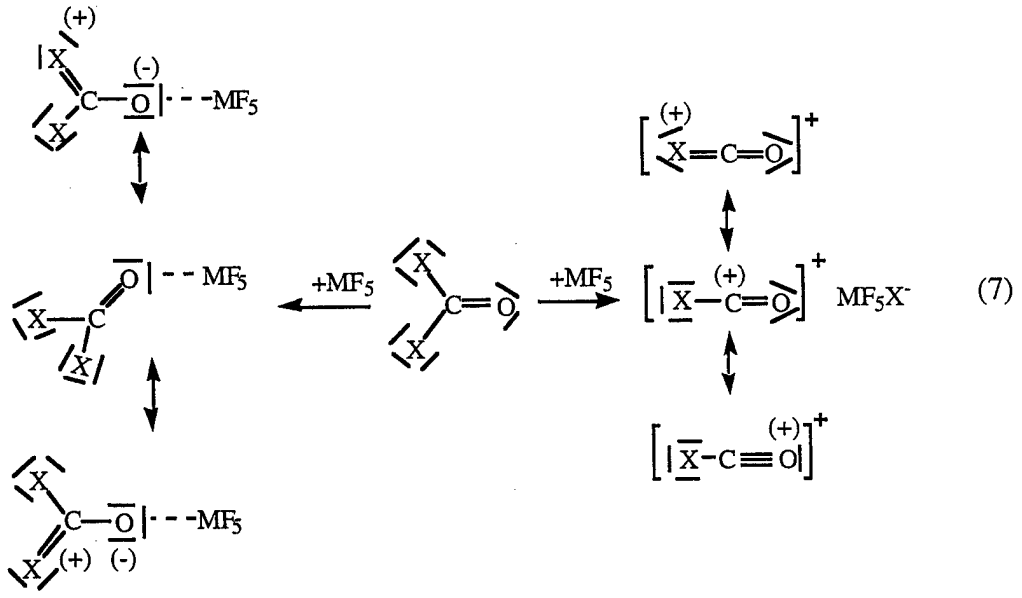

(7)

the C-O and the C-X bonds due to increased bond orders caused by electron back-donation from the ligands to the carbocation center, resulting in shifts to higher frequencies. In addition, the number of normal modes is reduced from 6 in X_2CO to three in XCO^+. On the other hand, for the oxygen-bridged, donor-acceptor adducts the bond order of the C-O bond is decreased, while that of the C-X bonds is increased. Furthermore, due to the additional bridge modes, the number of normal modes of the adduct is larger than the sum of the modes of the separate donor and acceptor molecules. The carbonyl stretching mode,which in ClFCO occurs at about 1868 cm^{-1},[36] is well separated from the other modes and, therefore, is ideally suited to distinguish the $ClCO^+$ cation from an oxygen-bridged, donor-acceptor adduct.

The observed low-temperature infrared and Raman spectra of $ClCO^+$ in $ClCO^+Sb_3F_{16}^-$ are summarized in Table 1. As can be seen, the carbonyl stretching mode of $ClCO^+$ is shifted by +388 cm^{-1} relative to ClFCO,[36] and by +592 cm^{-1} relative to the $ClFCO{\cdot}SbF_5$ donor-acceptor adduct, which has a carbonyl stretching frequency of 1664 cm^{-1}.[13] This huge frequency increase firmly establishes the presence of the $ClCO^+$ cation. Of the remaining two normal modes of $ClCO^+$ (linear $C_{\infty v}$ ClCO has two Σ stretching and one π bonding mode), the C-Cl stretching mode was observed at 803 cm^{-1}, whereas the bending mode is predicted by *ab initio* calculations (see below) and by comparison with the isoelectronic ClCN molecule,[37] to fall within the range of the anion modes and to have very low Raman intensity and, therefore, could not be located with confidence. Based on a private communication from Bernhardt, Willner and Aubke, who independently studied the vibrational spectra of $ClCO^+$, the deformation mode is observed in the infrared spectrum at 468 cm^{-1}.

Compared to ClFCO,[36] the C-Cl stretching frequency of $ClCO^+$ has also increased, as predicted above, although only by 27 cm^{-1}. The dramatic difference between the frequency

of F_2CO (1928 cm^{-1}),[36] and only the well known $F_2CO \cdot SbF_5$ donor-acceptor adduct with νC-O = 1770 cm^{-1} [10,13] was observed. This lack of evidence for FCO^+ formation agrees well with the results from the present NMR study.

Theoretical Calculations. High level *ab initio* calculations have previously been reported for $ClCO^+$,[39,40] FCO^+,[7] and isoelectronic ClCN[39] and FCN[41,42], the results of which were confirmed by the present work. Consequently, only the following six topics need to be discussed here.

(i) Vibrational Frequencies and ^{35}Cl-^{37}Cl Isotopic Shifts for $ClCO^+$. Harmonic ω and anharmonic (ν) frequencies, together with observed[37,42] and calculated data for isoelectronic ClCN, are summarized in Table 1. As can be seen, the CCSD(T)[39] results are in excellent agreement with the observed spectra. The observed ^{35}Cl-^{37}Cl isotopic shifts are also in accord with the calculations and clearly identify the vibrations involving a stretching of the C-Cl bond. The lower-level RHF calculations have also been included in Table 1 because they allowed the calculation of Raman intensities. As can be seen, the calculated Raman intensity of ν_2 of $ClCO^+$ is vanishingly small, explaining the absence of ν_2 in our Raman spectrum.

Force fields for $ClCO^+$ and ClCN at the CCSD(T)/cc-pVQZ level with frequencies very close to the experimentally observed ones have previously been published.[39] The force constants of greatest interest, f(CO) = 19.663 and f(CCl) = 6.455 mdyn/Å,[39] are in accord with a strong CO triple bond (f(CN) in ClCN = 17.720 mdyn/Å and f(CO) in CO = 18.56 mdyn/Å)[37,38] and a CCl bond with a bond order of 1.22, if the C-Cl bond in ClCN (f = 5.290 mdyn/Å)[38] is chosen as the basis for an *sp*-hybridized C-Cl single bond.

(ii) Predicted Geometry for $ClCO^+$. The excellent agreement of observed and calculated vibrational frequencies for $ClCO^+$ and comparison with the observed[43,44] and calculated structures

for ClCN (see Table 1), lend strong support to the previously proposed[39] geometry of r(CO) = 1.122 Å and r(CCl) = 1.567 Å for $ClCO^+$.

(iii) NMR Shifts. The calculated NMR chemical shifts of the isoelectronic $ClCO^+$/ClCN and FCO^+/FCN couples and $CFCl_3$ are summarized in Table 2 and compared to the experimentally observed shifts.[8,45] As can be seen, the agreement between the calculated and observed ^{13}C shifts of $ClCO^+$ is good, thus lending further support to the verification of $ClCO^+$. Table 2 also confirms the similarity of the ^{13}C shift of $CFCl_3$ and that previously attributed[9] to FCO^+.

(iv). Stabilization of the Carbocation Centers in the XCO^+ Cations and Natural Bond Order Analyses. The stability of carbocations is greatly enhanced by electron back-donation from a neighboring ligand, thus alleviating the electron deficiency of the carbenium center. This back-donation can occur either through the σ or *p-p-*π bonds. If the ligand is more electronegative than C^+, as is the case for fluorine, the σ back-donation becomes negative, i.e., the inductive effect of the fluorine ligand counteracts the p-p-π back-donation. Consequently, the total ($\sigma + \pi$) back-donation decreases with decreasing atomic weight of the halogen, i.e., I>Br>Cl>F. This point has recently been demonstrated by a natural bond order (NBO) analysis of the MX_3^+ and MH_2X^+ series, where M = C, Si, Ge, Sn, Pb and X = F, Cl, Br, I.[4] It was, therefore, worthwhile to extend this NBO analysis to FCO^+ and $ClCO^+$ and their isoelectronic species, in an effort to judge the relative contributions and the stabilizing or destabilizing effect of an oxygen ligand on the carbenium center. Calculations of atomic charge distributions frequently vary widely with the methods used, so they are not reliable predictors of quantities such as bond orders or back-donation, which are not physically observable. Nevertheless, an NBO analysis with the same basis sets should correctly reflect trends within a given series. For more quantitative

comparisons, bond distances or reliable force constants should be used, provided that they are corrected for secondary effects such as differences in the hybridization of the binding electrons.

In Frenking's NBO analysis[4] of CF_3^+, the degree of p(π) back-donation from F to C was obtained by assuming the ideal carbenium resonance structure with an empty p(π) orbital

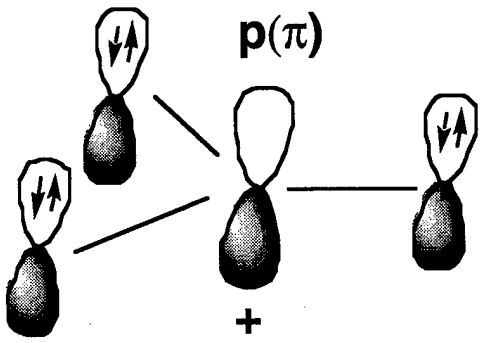

and the full positive charge being on carbon, while the three fluorines are σ-bonded through sp_2 hybridization. The p(π) back-donation from C to F was obtained by calculating for the minimum energy structure the actual p(π) population on carbon and dividing it by three to obtain the p(π) back-donation from each fluorine ligand. From this value and the calculated atomic charge distribution, the σ-donation can be calculated according to (8).

$$\text{atomic charge} = p(\pi) - \sigma \qquad (8)$$

The results can best be summarized using simple arrow diagrams in combination with charge distributions, as shown in (9) and (10) for CF_3^+, and CCl_3^+, respectively.

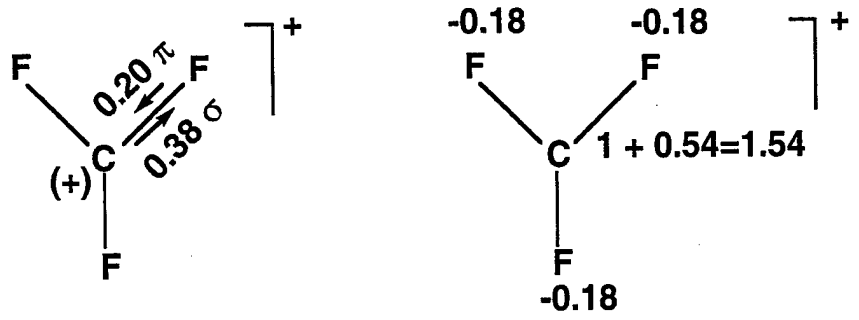

(9)

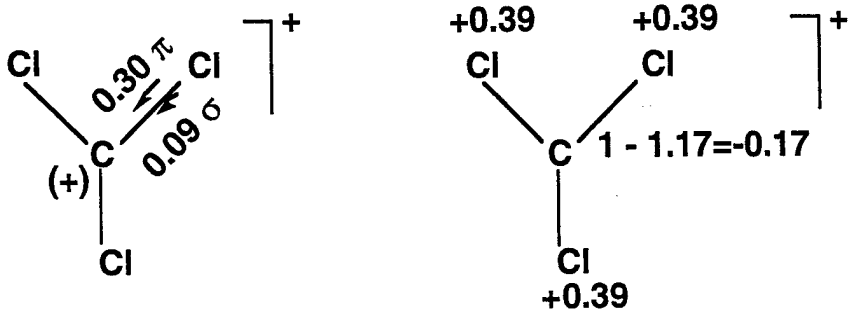

(10)

Since CF_3^+ and CCl_3^+ are singly charged cations, the sum of their atomic charge distributions must equal +1. As can be seen from (9) and (10), the p(π) back-donation increases from fluorine to chlorine, but the most dramatic effect is caused by the large change and sign reversal of the σ-donation, which is caused by fluorine being more and chlorine being less electronegative than C^+. This strong negative σ-effect of fluorine also preempts fluorine from acquiring a positive atomic charge, as might be implied from the simple fluoronium valence bond description (+) $\langle$F=C=O$\rangle$.

Extension of this NBO analysis to isoelectronic BF_3 (11) furthermore demonstrates that

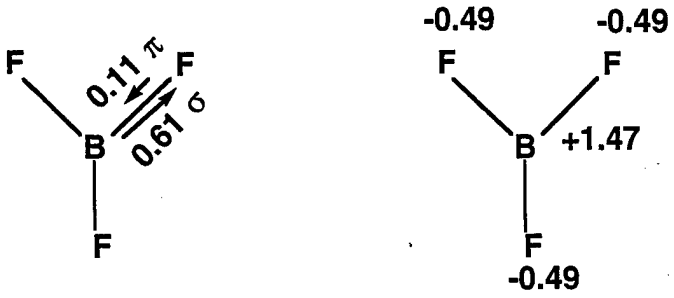

(11)

$p(\pi)$ back-donation in BF_3 is even smaller than in CF_3^+. In view of the excellent stability of BF_3, insufficient $p(\pi)$ back-donation in CF_3^+ cannot be blamed for the elusiveness of CF_3^+ in the condensed phase.

Extension of the NBO analyses to the halocarbonyl cations causes complications, because their two ligands are different and the second and third bonds of the carbonyl group are π-bonds. The following general approach successfully overcomes these complications: (i) all sp_n orbitals, which are required for the σ-bonded backbone, must be kept occupied, while all $p(\pi)$ orbitals on the carbon central atom must be vacated and their electrons be transferred to the ligands; (ii) the $p(\pi)$ back-donation from each ligand is calculated by subtracting its actual $p(\pi)$ orbital population from its fully occupied population value; and (iii) the σ-donation from the central atom to the ligand is calculated by substracting the atomic charge from the $p(\pi)$ back-donation, under consideration of the formal charges generated by the vacating of the $p(\pi)$ orbitals on the central atom.

The FCO^+ cation is used to exemplify this approach.

Step (i): All $p(\pi)$ orbitals on carbon are vacated and their electrons transferred to the ligands, which generates the electron distributions and formal charges shown in (12).

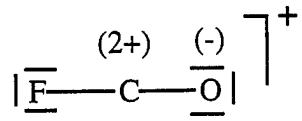

(12)

Step (ii): The following $p(\pi)$ orbital populations were obtained from the *ab-initio* calculations:

F:	p_x	1.84883	3.69766
	p_y	1.84883	
C:	p_x	0.68429	1.36858
	p_y	0.68429	
O:	p_x	1.43242	2.86484
	p_y	1.43242	
	$\Sigma p_x + p_y$ =		7.93108

Due to a small percentage of the electrons occupying higher orbitals or Rydberg states, the above sum of 7.93 electrons in the p_x and p_y orbitals is only 99.14% of the possible 8.0. Consequently, the fully occupied $(p_x + p_y)\pi$ orbital population values on fluorine and oxygen in (12) must be normalized by 0.9914, giving 4 x 0.9914 = 3.96554 electrons. The third free valence electron pairs on fluorine and oxygen can be ignored because they are p_Z-σ pairs which cannot participate in the π-bonding. Subtraction of the above calculated $(p_x + p_y)$ orbital population from the fully populated orbitals results in the following $p(\pi)$ back-donation values:

F: 3.96554 - 3.69766 = 0.26788 electrons

O: 3.96554 – 2.86484 = 1.10070 electrons

Step (iii): The calculated atomic charge distributions in FCO^+ are:

$$\left[\begin{array}{ccccc} F & \text{———} & C & \text{———} & O \\ -.10247 & & +1.26659 & & -.16412 \end{array}\right]^+ \qquad (13)$$

Substraction of the atomic charge values from the sum of the formal charges on the specific ligands in (12) and the p(π) back-donation values calculated in step (ii) results in the following σ-donation from carbon to the ligands:

F: 0.26788 + .10247 = 0.37035 electrons

O: -1.00000 + 1.10070 + .16412 = 0.26482 electrons

Using a simple arrow diagram to better visualize the π- and σ-donation effects and the resulting atomic charges, (13) can be rewritten in the following manner (14), where the lengths of the arrows reflect the directions and magnitudes of the values:

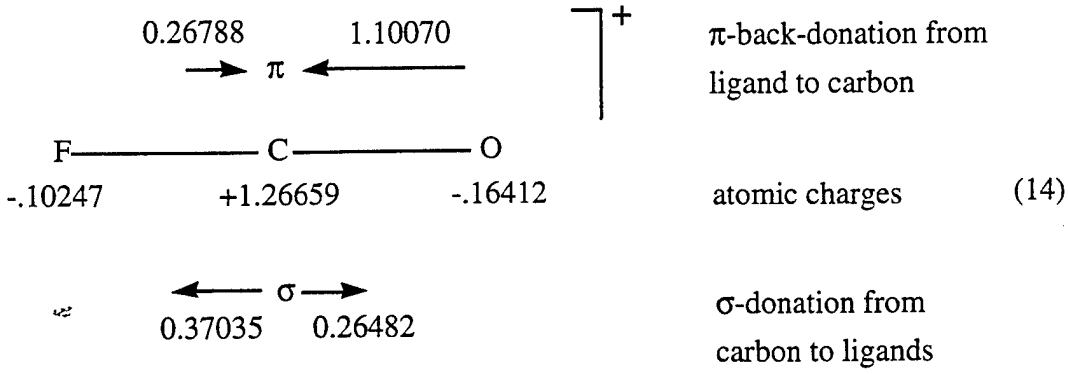

The veracity of the above procedure can easily be crosschecked by starting with the formal charges on each atom in (12) and correcting them for the σ-donations and p(π) back-donations; the result must equal the calculated atomic charges.

The results of our QCISD/6-311+G(2d) NBO analyses for FCO^+, $ClCO^+$ and their isoelectronic counterparts FCN and ClCN are summarized in Table 3. They show that chlorine is a better p(π) back-donor than fluorine, and oxygen is a much better p(π) back-donor than the halogens. This results in full triple bonds for the C-O and C-N bonds, but does not generate a positive atomic charge on oxygen, as the simple valence bond description, $|\underline{\overline{F}}-C\equiv\overset{(+)}{O}|$, would require, thus demonstrating the potential fallacy of atomic charges derived solely from valence

unfavorable. Therefore, the problem of preparing condensed state CF_3^+ salts is attributed to a combination of unfavorable overall thermodynamics (endothermicity of (15) and high activation energy for breakage of the very strong C-F bond in CF_4) and the lack of stable alternate starting materials, such as difluorocarbene, which could be oxidatively fluorinated with compounds, such as XeF^+ or N_2F^+. For a successful CF_3^+ salt synthesis a Lewis acid will be required whose F^- affinity exceeds that of SbF_5 by at least 20-30 kcal/mol. This estimate is based on the sum of the 19 kcal/mol endothermicity of (18) and the extrapolated 11 kcal/mol exothermicity of the competing formation of the oxygen-bridged, $F_2CO{\cdot\cdot}SbF_5$, donor-acceptor complex.[13] Since SbF_5 has the highest known fluoride ion affinity,[49] it appears unlikely that a substantially stronger Lewis acid can be found.

Analogous Born-Haber cycles for (16) and (17) give estimates of about 4 and –12 kcal/mol, respectively. Considering that the dissociation enthalpies of oxygen bridged donor-acceptor adducts, such as $ClFCO{\cdot}SbF_5$, are about 10-15 kcal/mol for SbF_5 adducts and 15-25 kcal/mol for AsF_5 adducts, it is then not surprising that the oxygen bridged donor-acceptor adducts are favored over the ionic adducts. Even for ClFCO, the use of a single SbF_5 molecule is still insufficient to produce $ClCO^+SbF_6^-$, and at least three SbF_5 molecules must be used to form $ClCO^+Sb_3F_{16}^-$ by increasing the F^- affinity of the Lewis acid and by decreasing the depolymerization enthalpy[48] of liquid SbF_5. Apparently, these effects outweigh the decrease in lattice energy, expected for the increased molecular volume.[50] The same arguments hold for the Cl_2CO/SbF_5 system where an analogous Born-Haber cycle estimate shows the formation of the oxygen bridged donor-acceptor adduct to be favored by about 10 kcal/mol over that of the ionic $ClCO^+SbF_5Cl^-$ salt.

(vi). Theoretical Evaluations of the SbF_5 + ClFCO and Sb_3F_{15} + ClFCO Systems. The interaction of ClFCO with a strong Lewis acid, such as SbF_5, represents the very interesting case of a donor molecule possessing three competing donor sites, i.e., oxygen, fluorine and chlorine. In the case of an attractive halogen interaction, a complete transfer of one halogen to the Lewis acid under formation of a halocarbonyl cation and an SbF_5X^- anion could occur. Further interest stems from the observation that SbF_5 forms with ClFCO only an oxygen-bridged donor-acceptor adduct, whereas Sb_3F_{15} forms an ionic $ClCO^+Sb_3F_{16}^-$ salt. It was, therefore, desirable to investigate whether such a complex system could be modeled and predicted correctly by theoretical methods.

In view of the relatively large size of the molecules involved, density functional methods and effective core potentials (B3LYP/SBK+(d)) were used for our calculations.[30-33] For the SbF_5/ClFCO system a sequence of constrained optimizations were performed in which the distance between the Sb atom and the F atom on ClFCO was held fixed while the remaining geometrical degrees of freedom were fully optimized. Similar calculations were also carried out in which the Sb-Cl and Sb-O distances were likewise fixed. The energy profiles as a function of the fixed Sb-F, Sb-Cl, and Sb-O distances are shown in Figure 1, and selected optimized geometries for each approach are shown in Figures 2-5. Figure 1 indicates that the potential energy curves for chlorine- and for fluorine-bridging are repulsive and do not show a minimum, with the chlorine curve being more repulsive than that for fluorine. Furthermore, the carbonyl halide groups in the fluorine- and the chlorine-bridged structures do not lie in the paper planes of Figures 2 and 3, but form dihedral angles ranging from about 80 to 130° with respect to the paper planes, resulting in C_1 symmetry. The corresponding Cs symmetry structures, in which the

carbonyl halide ligands lie in the paper planes of Figures 2 and 3 are about 1 kcal/mol higher in energy.

For the oxygen-bridged $ClFCO \cdot SbF_5$ adduct, Figure 1 shows a shallow minimum, in agreement with the experimental finding of a weak donor-acceptor adduct. In this adduct, the two halogen ligands of the ClFCO group lie in the paper planes of Figures 4 and 5, resulting in C_s symmetry. The structure in which the fluorine ligand of ClFCO points towards the SbF_5 group (Fig. 4) is only slightly lower (by 0.03 kcal/mol for R(Sb-O)=2.40 Å) in energy than that of Figure 5, and their geometries are very similar.

Analogous calculations were also done for the Sb_3F_{15} + ClFCO system, in which the distance between the central Sb atom in Sb_3F_{15} and the F, Cl, or O atom of ClFCO was held fixed, with the resulting energy curves shown in Figure 6. The chlorine-bridged approach was again repulsive, and a typical geometry for one of the points on the curve is shown in two different perspectives in Figure 7. Other configurations, with the fluorine ligand of ClFCO pointing up or the COClF group being rotated by 180°, i.e., pointing away from the Sb_3F_{15} group, were found to be higher in energy by 1.67 and 3.6 kcal/mol, respectively, for R(Sb-Cl)=2.30 Å.

For the oxygen-bridged approach of Sb_3F_{15} by ClFCO a shallow minimum was found for its potential energy curve (see Figure 6), indicative of a marginally stable donor-acceptor adduct. Figure 8 shows two perspectives of its minimum energy geometry. As can be seen, this adduct has a symmetry plane, i.e., symmetry C_s. Other geometries, such as the ones shown in Figure 9, were also explored, but found to be higher in energy by about 1-2 kcal/mol.

The fluorine-bridged approach of Sb_3F_{15} by ClFCO results in a well defined minimum, corresponding to the transfer of a fluoride ion from ClFCO to Sb_3F_{15} with formation of the ionic salt $ClCO^+$ $Sb_3F_{16}^-$ (see Figure 10). The small local maximum at about 2.1Å in the F-approach

potential of Figure 6 is indicative of a small barrier due to the breaking of the C-F bond, which is required for the fluoride ion transfer. Although the minimum for the oxygen-bridged $ClFCO{\cdot}Sb_3F_{15}$ adduct is about 12 kcal/mol lower than that for the ionic $ClCO^+$ $Sb_3F_{16}^-$ ion pair, it must be kept in mind that these potentials are for the free gaseous species. In the condensed phase, the larger lattice energy of the ionic form lowers its energy well below that of the oxygen-bridged donor-acceptor adduct and confirms the experimental finding of the ionic salt.

These computations demonstrate that it is possible to predict correctly not only the preferred coordination site, i.e., oxygen versus fluorine versus chlorine, but also whether a covalent oxygen-bridged, donor-acceptor complex is favored over an ionic complex, which can emanate from a halogen-bridge. Our calculations also correctly predict that SbF_5 is not sufficiently acidic to remove a fluoride ion from ClFCO, but Sb_3F_{15} can do so. Furthermore, they confirm the conclusions and rough energy estimates derived from the Born-Haber cycles.

Conclusions

Our experimental and computational studies show that with the presently known Lewis acids the synthesis of condensed phase CF_3^+ salts cannot be achieved due to unfavorable overall thermodynamics. For FCO^+ salts, the situation becomes somewhat more favorable, but the formation of covalent, oxygen-bridged, donor-acceptor complexes between F_2CO and the Lewis acids is still clearly favored, and the previous claim for the observation of FCO^+ in solution by NMR spectroscopy could not be confirmed. For ClFCO, the formation of either $ClCO^+$ salts or oxygen-bridged, ClFCO·Lewis acid, donor-acceptor adducts was observed, depending on the strength of the Lewis acid used. Computational methods were used to calculate the extent of σ-donation and p(π) back-donation in compounds containing more than one type of ligand, and

References

Loker Hydrocarbon Research Institute, University of Southern California, Los Angeles, California.

§ Air Force Research Laboratory, Edwards Air Force Base, California

† Present Address: Institute of Inorganic Chemistry, University of Cologne, Germany

(1) Olah, G. A. *Friedel-Crafts Chemistry*, Wiley, New York, **1973**.

(2) Olah, G. A. *Carbocations and Electrophilic Reactions*, Verlag Chemie, John Wiley & Sons, New York, **1973**.

(3) *Stable Carbocation Chemistry*; Prakash, G. K. S., Schleyer, P. v. R., EDS; John Wiley & Sons, New York, **1997**.

(4) Frenking, G.; Fau, S.; Marchand, C. M.; Grützmacher, H. *J. Am. Chem. Soc.* **1997**, *119*, 6648.

(5) Martin, R. H.; Lampe, F. W.; Taft, R. W. *J. Am. Chem. Soc.* **1966**, *88*, 1353.

(6) Olah, G. A.; Rasul, G.; Heiliger, L.; Prakash, G. K. S. *J. Am. Chem. Soc.* **1996**, *118*, 3580; Olah, G. A.; Heiliger, L.; Prakash, G. K. S. *J. Am. Chem. Soc.* **1989**, *111*, 8020.

(7) Botschwina, P.; Sebald, P.; Bogey, M.; Demuynck, C.; Destombes, J.-L. *J. Mol. Spectrosc.* **1992**, *153*, 255.

(8) Prakash, G. K. S.; Bausch, J. W.; Olah, G. A. *J. Am. Chem. Soc.* **1991**, *113*, 3203.

(9) (a) Olah, G. A.; Burrichter, A.; Mathew, T.; Vankar, Y.D.; Rasul, G.; Prakash, G. K. S. *Angew. Chem. Int. Ed. Engl.* **1997**, *36*, 1875; (b) Sorensen, T. S. *Angew. Chem. Int. Ed. Engl.* **1998**, *37*, 603.

(10) Chen, G. S. H.; Passmore, J. *J. C. S. Dalton* **1979**, 1257.

(11) Christe, K. O. *Inorg. Chem.* **1967**, *6*, 1706.

K.; Rozyczko, P.; Sekino, H.; Hober, C.; Bartlett, R. J. Integral packages included are VMOL. Almlof, J.; Taylor, P. R.; BPROPS Taylor, P. R.; and ABACUS Helgaker, T.; Jensen, H. J. Aa.; Jorgensen, P.; Olsen, J.; Taylor, P. R.

(27) Reed, A.E.; Curtiss, L. A.; Weinhold, F. *Chem. Rev.* **1988**, *88*, 1899.

(28) Pople, J. A.; Head-Gordon, M.; Raghavachari, K. *J. Chem. Phys.* **1987**, *87*, 5968.

(25) (a) Gaussian 94, Revision E. 2, Frisch, M.J.; Trucks, G. W.; Schlegel, H. B.; Gill, P. M. W., Johnson, B. G.; Robb, M. A.; Cheeseman, J. R.; Keith, T.; Petersson, G. A.; Montgomery, J. A.; Raghavachari, K.; Al-Laham, M. A.; Zakrzewski, V. G.; Ortiz, J. V.; Foresman, J. B.; Cioslowski, J.; Stefanov, b. b.; Nanayakkara, A.; Challacombe, M.; Peng, C. Y.; Ayala, P. Y.; Chen, W.; Wong, M. W.; Andres, J. L.; Replogle, E. S.; Gomperts, R.; Martin, R. L.; Fox, D. J.; Binkley, J. S.; Defrees, D. J.; Baker, J.; Stewart, J. P.; Head-Gordon, M.; Gonzalez, C.; and Pople, J. A.; Gaussian, Inc., Pittsburgh, PA, 1995. (b) NBO Version 3.1, Glendening, E. D.; Reed, A. E.; Carpenter, J. E.; Weinhold, F.

(30) Becke, A. D. *J. Chem. Phys.* **1993**, *98*, 5648.

(31) a. Melius, C. F.; Goddard, W. A. *Phys. Rev. A.* **1974**, *10*, 1528.

b. Kahn, L. R.; Baybutt, P.; Truhlar, D. G. *J. Chem. Phys.* **1976**, *65*, 3826.

c. Krauss, M.; Stevens, W. J. *Ann. Rev. Phys. Chem.* **1985**, *35*, 357.

d. Stevens, W. J.; Basch, H; Krauss, M. *J. Chem. Phys.* **1984**, *81*, 6026.

e. Stevens, W. J.; Basch, H.; Krauss, M.; Jasien, P. *Can. J. Chem.* **1992**, *70*, 612.

f. Cundari, T. R.; Stevens, W. J. *J. Chem. Phys.* **1993**, *98*, 5555.

(32) The diffuse s+p function exponents used for Sb, Cl, F, O, and C were 0.0259, 0.0483, 0.1076, 0.0845, and 0.0438, respectively.

(33) The d function exponents used for Sb and Cl were 0.211 and 0.75, respectively. An exponent of 0.8 was used for F, O, and C.

(34) Dean, P. A. W.; Gillespie, R. J. *J. Am. Chem. Soc.* **1969**, *91*, 7260.

(35) Lindquist, I. "Inorganic Adduct Molecules of Oxo-Compounds," Anorganische und Allgemeine Chemie in Einzeldarstellungen, Band IV, Becke-Goehring, M. Ed.; Academic Press Inc., New York, **1963**.

(36) Shimanouchi, T. *J. Phys. Chem. Ref. Data* **1977**, *6*, 993, and references cited therein.

(37) Shimanouchi, T. "Tables of Molecular Vibrational Frequencies, Consolidated Volume 1," NSRDS-NBS39, *Nat. Stand. Ref. Data Ser., Nat. Bur. Stand.* (U. S.), **1972**, and references cited therein.

(38) Siebert, H. "Anwendungen der Schwingungsspektroskopie in der Anorganischen Chemie," Anorganische und Allgemeine Chemie in Einzeldarstellungen, Band VII, Becke-Goehring, M. Ed.; Springer Verlag, Berlin Heidelberg, New York, **1966**.

(39) Pak, Y.; Woods, R. C. *J. Chem. Phys.* **1997**, *107*, 5094.

(40) Peterson, K. A.; Mayrhofer, R. C.; Woods, R. C. *J. Chem. Phys.* **1991**, *94*, 431.

(41) Lee, T. J.; Racine, S. C. *Mol. Phys.* **1995**, *84*, 717.

(42) Lee, T. J.; Martin, J. M. L.; Dateo, C. E.; Taylor, P. R. *J. Phys. Chem.* **1995**, *99*, 15858.

(43) Lafferty, W. J.; Lide, D. R.; Toth, R. A. *J. Chem. Phys.* **1965**, *43*, 2063.

(44) Saouli, A.; Dubois, I.; Blavier, J. F. Bredohl, H.; Blanquet, G.; Meyer, C.; Meyer, F. *J. Mol. Spectrosc.* **1994**, *165*, 349.

(45) Fawcett, F. S.; Lipscomb, R. D. *J. Am. Chem. Soc.* **1960**, *82*, 1509, and **1964**, *86*, 2576.

(46) Walker, N.; Fox, W. B.; De Marco, R. A.; Moniz, W. B. *J. Magn. Reson.* **1977**, *27*, 345.

Table 1: Observed and Calculated Vibrational Spectra and Bond Lengths of $ClCO^+$ and Isoelectronic ClCN

assgnts and approx mode descriptions in point group $C_{\infty v}$	obsd freq, cm^{-1}(rel intens)				calcd freq, cm^{-1} (IR int) [RA int][a]					
	$ClCO^+Sb_3F_{16}^-$		ClCN[b]		$ClCO^+$				ClCN	
	IR	RA[c]	IR(gas)	RA(liq)[c]	RHF[d]	CCSD(T)[d]	CCSD(T)/cc-pVQZ		CCSD(T)[d]	CCSD
					ω	ω	ω	ν	ω	ω
$\upsilon_1(\Sigma)$ C≡Y stretch (^{35}Cl)	2256vs	2256(10)	2215.6vs	2206(10)	2601.3 (505) [40.6]	2258(258)	2289.2	2256.7	2220(19)	2242
C≡Y stretch (^{37}Cl)			2215.3vs		2601.1 (505) [40.6]					
$\upsilon_2(\pi)$ ^{35}Cl-C≡Y bend	e	not obsd	378.4s	394(3)	521.3 (27) [0]	472(21)	478.6	475.4	375(4)	382
^{37}Cl-C≡Y bend			378.0s		520.7 (28) [0]					
$\upsilon_3(\Sigma)$ ^{35}Cl-C stretch	802.5s	803(8)	744.2[f]s	730(5)	821.6 (33) [1.8]	773(28)	807.4	789.6	714(7)	
^{37}Cl-C stretch	793.8m	794(3)	736.0s		811.8 (33) [1.8]					
$(\upsilon_1 + \upsilon_3)(\Sigma)$ ^{35}Cl	3056.1mw									
^{37}Cl	30470w									
bond lengths										
r(C-Cl)			1.6297[h]		1.581	1.589		1.574	1.657	
r(C-X)			1.1596		1.089	1.128		1.125	1.165	

[a] Infrared intensities in km/mol; Raman intensities in $Å^3$/amu. [b] Data from ref 37 and 43. [c] Uncorrected Raman intensities. [d] A 6-311 + G* basis set was used for these calculations. [e] Obscured by $Sb_3F_{16}^-$ bands. [f] In the Ir spectrum, this band is split by Fermi resonance with $2\nu_2$ into two intense bands at 782.6 and 714.0 cm^{-1}. [g] Data from ref 39. [h] Data from ref 44.

Table 3. Results from the NBO Analyses at the 2CISD/6-311+G(2d) Level for FCO^+, $ClCO^+$, FCN and ClCN. The Left Column shows the p(π) Back-Donation from the Ligands to the Carbon Atom, the σ-Donation from Carbon to the Ligands, and the Formal Charges Generated by vacating all p(π) Orbitals on Carbon; the Right Column gives the Atomic Charge Distributions and Calculated Bond Distances.

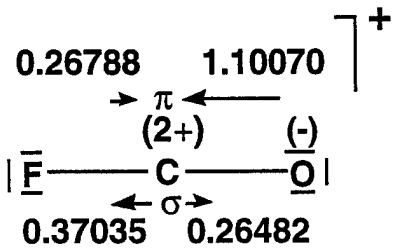

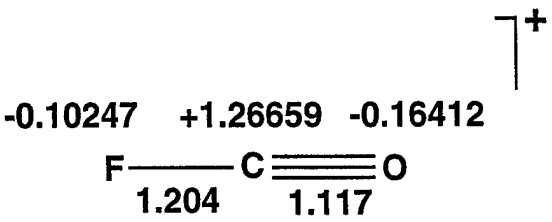

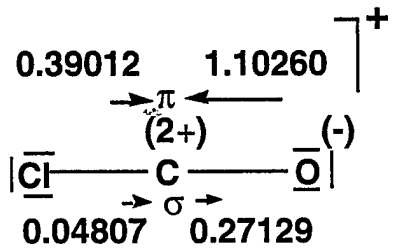

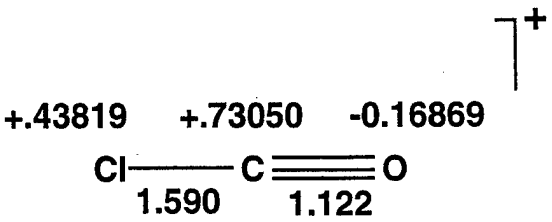

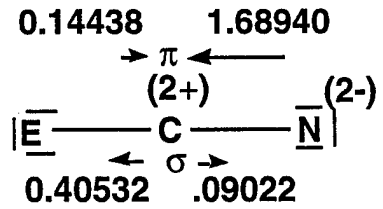

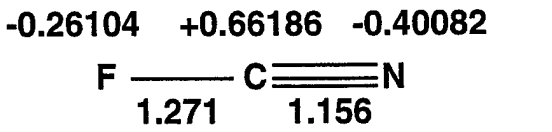

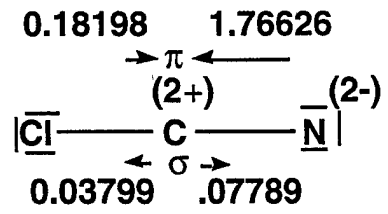

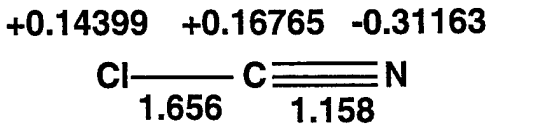

Diagram Captions

Figure 1. B3LYP/SBK+(d) constrained optimizations for the fluorine-, chlorine-, and oxygen-bridged interactions of ClFCO and SbF_5. The Sb-F, Sb-Cl and Sb-O distances were fixed at the indicated R values.

Figure 2. Optimized geometries for three points on the potential energy curve of Figure 1 for the fluorine-bridged approach of SbF_5 by ClFCO. The dihedral angle w is defined as the angle which the ClCO plane forms with respect to the SbFC plane. Color code: green = Cl, red = O, grey = C, light blue = F, dark blue = Sb.

Figure 3. Optimized geometries for three points on the potential energy curve of Figure 1 for the chlorine-bridged approach of SbF_5 by ClFCO.

Figure 4. Optimized geometry of the oxygen-bridged $ClFCO \cdot SbF_5$ adduct with a fixed Sb-O bond length of 2.40Å and the chlorine atom pointing away from the SbF_5 group.

Figure 5. Optimized geometries for three points on the potential energy curve of Figure 1 for the oxygen-bridged approach of SbF_5 by ClFCO with the chlorine atom pointing towards the SbF_5 group.

Figure 6. B3LYP/SBK+(d) constrained optimizations for the fluorine-, chlorine-, and oxygen-bridged interactions of ClFCO and Sb_3F_{15}. The Sb-F, Sb-Cl and Sb-O distances were fixed at the indicated R values.

Figure 7. Two perspectives of the optimized geometry for the chlorine-bridged approach of Sb_3F_{15} by ClFCO at R(Sb-Cl)=2.20Å.

Figure 8. Two perspectives of the optimized geometry for the oxygen-bridged approach of Sb_3F_{15} by ClFCO at R(Sb-O)=2.17 Å.

Figure 9. Relative energies (in kcal/mol) of four different optimized geometries for the oxygen-bridged approach of Sb_3F_{15} by ClFCO.

Figure 10. Optimized geometries for three points on the potential energy curve of Figure 6 for the fluorine-bridged approach of Sb_3F_{15} by ClFCO, resulting in complete transfer of a fluoride ion from ClFCO to Sb_3F_{15}.

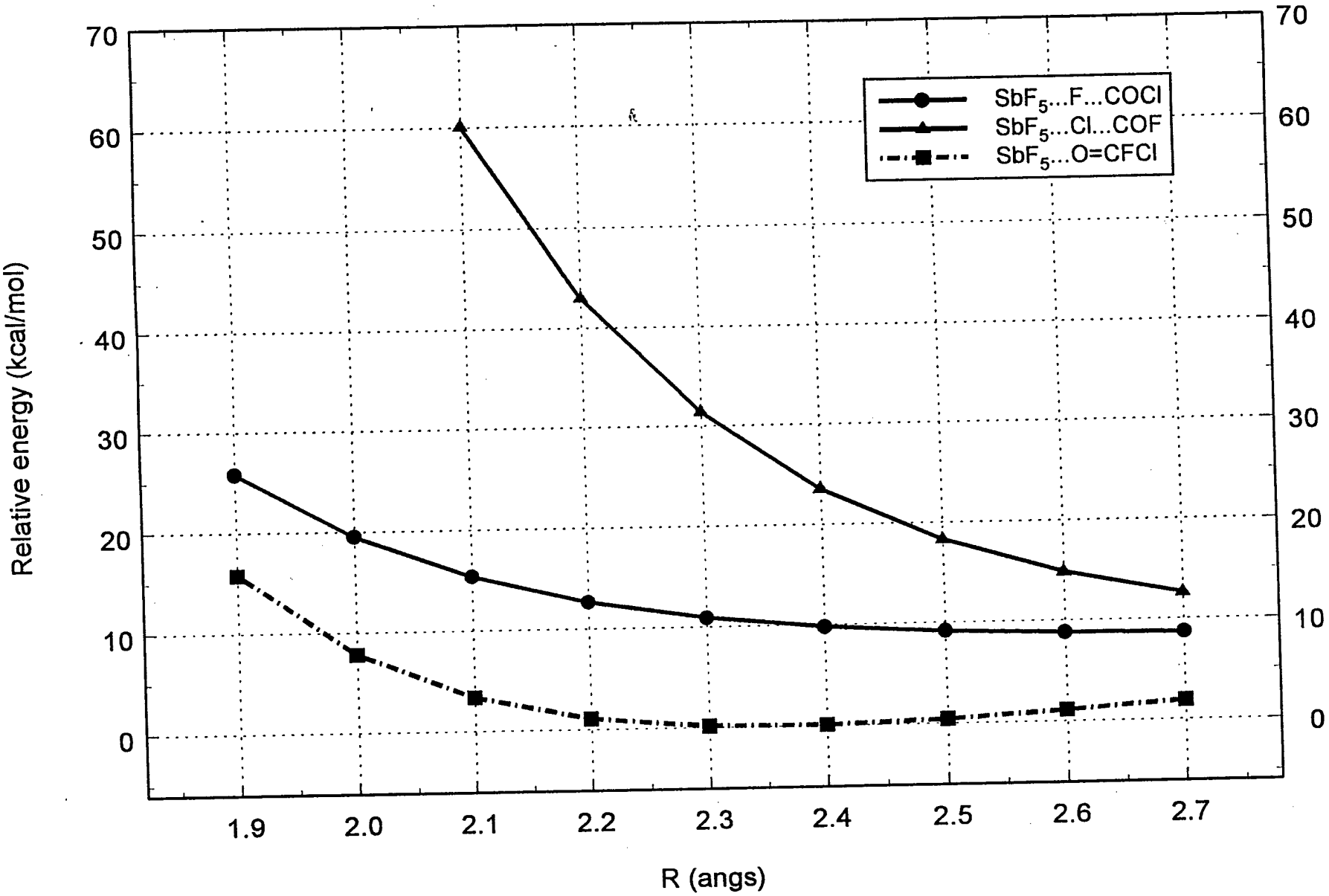
Relative energy (kcal/mol)
70
60
50
40
30
20
10
0
1.9
2.0
2.1
2.2
2.3
2.4
2.5
2.6
2.7
R (angs)
SbF5...F...COCl
SbF5...Cl...COF
SbF5...O=CFCl

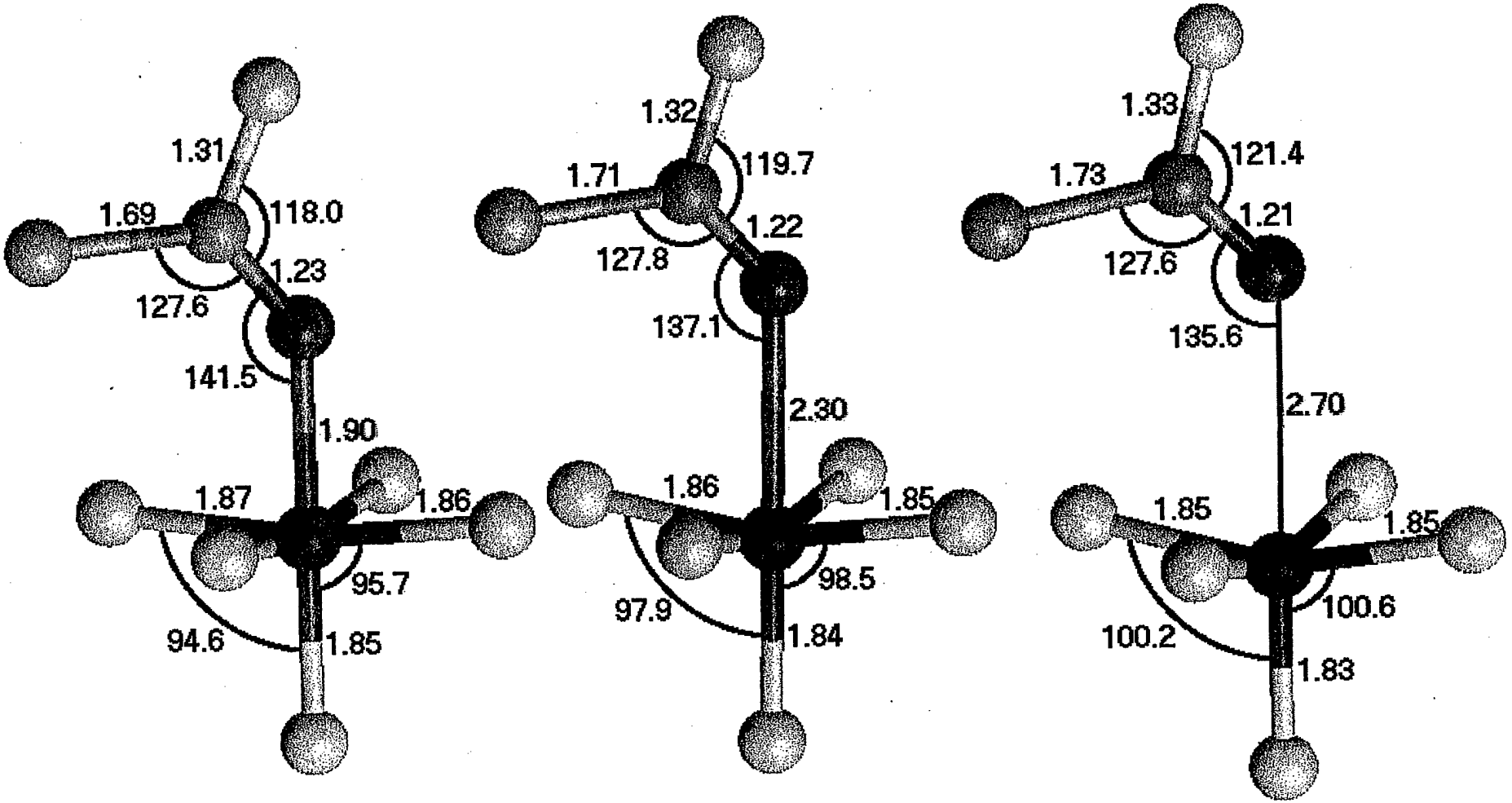
1.31
1.69
118.0
1.23
127.6
141.5
1.90
1.87
1.86
95.7
94.6
1.85
1.32
1.71
119.7
1.22
127.8
137.1
2.30
1.86
1.85
98.5
97.9
1.84
1.33
1.73
121.4
1.21
127.6
135.6
2.70
1.85
1.85
100.6
100.2
1.83

Fig. 5

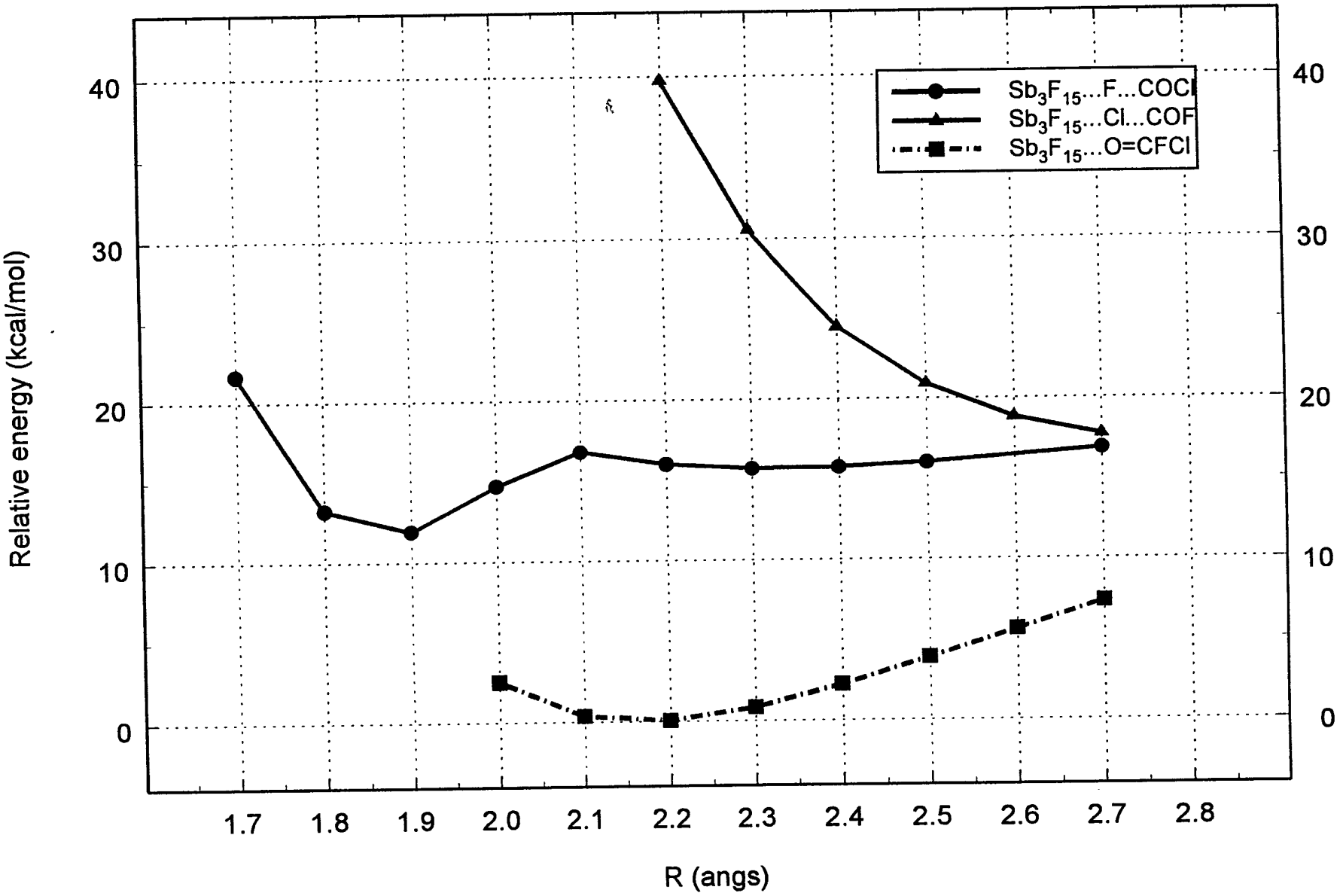
Relative energy (kcal/mol)
40
30
20
10
0
1.7
1.8
1.9
2.0
2.1
2.2
2.3
2.4
2.5
2.6
2.7
2.8
R (angs)
Sb_3F_{15}...F...COCl
Sb_3F_{15}...Cl...COF
Sb_3F_{15}...O=CFCl

Fig. 6

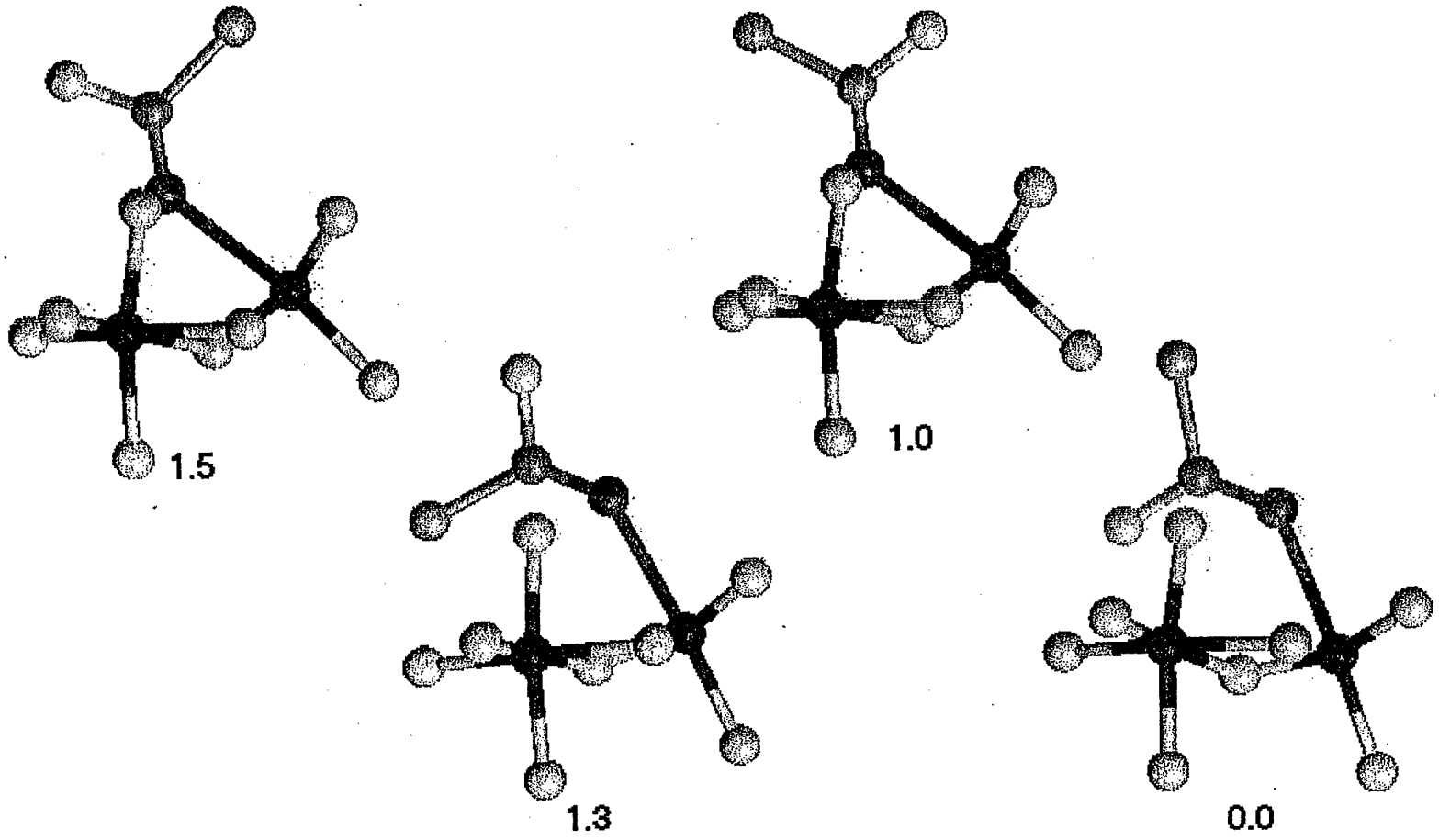

FIGURE 9

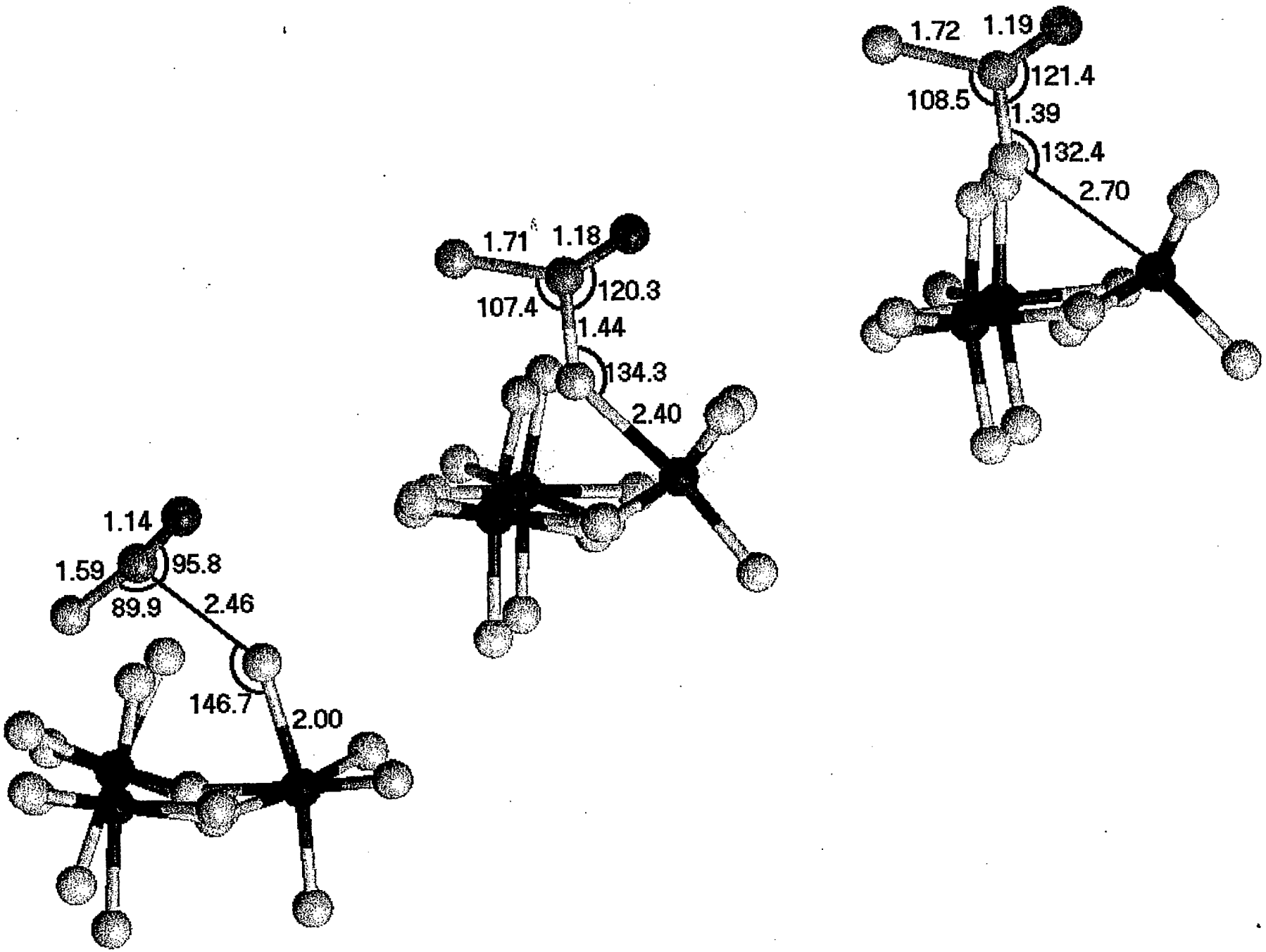
1.72
1.19
121.4
108.5
1.39
132.4
2.70
1.71
1.18
120.3
107.4
1.44
134.3
2.40
1.14
1.59
95.8
89.9
2.46
146.7
2.00

FIGURE 10